Mass analyzed threshold ionization spectra of phenol···Ar2: ionization energy and cation intermolecular vibrational frequencies

Antonio Armentano,[ac] Xin Tong,[ac] Mikko Riese,[abc] Simon M. Pimblott,[abc] K. Müller-Dethlefs,*[ac] Masaaki Fujii*[d] and Otto Dopfer*[e]

The phenol$^+$···Ar2 complex has been characterized in a supersonic jet by mass analyzed threshold ionization (MATI) spectroscopy *via* different intermediate intermolecular vibrational states of the first electronically excited state (S1). From the spectra recorded *via* the S1$0^0$ origin and the S1β_x intermolecular vibrational state, the ionization energy (IE) has been determined as $68\,288 \pm 5$ cm^{-1}, displaying a red shift of 340 cm^{-1} from the IE of the phenol$^+$ monomer. Well-resolved, nearly harmonic vibrational progressions with a fundamental frequency of 10 cm^{-1} have been observed in the ion ground state (D0) and assigned to the symmetric van der Waals (vdW) bending mode, β_x, along the x axis containing the C–O bond. MATI spectra recorded *via* the S1 state involving other higher-lying intermolecular vibrational states (σ_s^1, β_x^3, $\sigma_s^1\beta_x^1$, $\sigma_s^1\beta_x^2$) are characterized by unresolved broad structures.

1. Introduction

Clusters composed of aromatic molecules and rare gas atoms are ideal model systems to characterize the intermolecular interaction of non-polar solvent molecules with the highly polarisable aromatic π electron system. Of particular interest is the effect of the substitution of functional groups and the charge state on the interaction potential.[1] To this end, a variety of van der Waals (vdW) complexes of monosubstituted benzene molecules with argon have been investigated in their neutral electronic ground and excited states (S0, S1) as well as the cation ground state (D0) by resonant enhanced multi-photon ionization (REMPI) spectroscopy and the two equivalent spectroscopic methods for the investigation of the threshold ionization, namely mass analyzed threshold ionization (MATI) and zero kinetic energy (ZEKE) spectroscopy. These techniques provide essential information of the intermolecular interaction potential, including structure and intermolecular vibrational frequencies. Previous examples of A$^{(+)}$···Ar$_n$ clusters with aromatic molecules include A = benzonitrile,[2,3] fluorobenzene,[4,5] and aniline.[6–10]

Phenol is another fundamental mono-substituted benzene molecule with an electron donor group (OH) and two principle binding sites for neutral ligands. One interaction can be established with the substituent by the formation of a hydrogen bond to the OH group and the other binding motif

corresponds to a van der Waals interaction with the aromatic π-electron system. A large numbers of spectroscopic investigations supported by computational methods provide information on the phenol···Ar$_n$ structures ($n \leq 2$) in the S0, S1, and D0 electronic states. REMPI,[11] infrared (IR)[12] and Raman[13] spectroscopy suggested that π-bonding between Ar and phenol is the only possible interaction motif in the neutral S0 and S1 states. Recent high-level *ab initio* quantum chemical calculations[14] also support a π-bonded global minimum, whereas the H-bound structure is only a transition state in the S0 state. Hole-burning spectroscopy of phenol···Ar$_n$ with $n = 1$ and 2 demonstrated that only one isomer is present in the molecular beam expansion.[15] Subsequent high-resolution rotationally resolved laser induced fluorescence spectra have confirmed that phenol···Ar and phenol···Ar2 have π-bonded equilibrium structures, with Ar atoms located at opposite sides of the aromatic ring.[16]

MATI,[17] ZEKE,[18] photoionization efficiency (PIE),[19] and IR spectroscopy[20] are consistent with a π-bonded phenol$^+$···Ar structure also in the cation ground state. In contrast, the IR photodissociation spectrum of phenol$^+$···Ar generated in an electron impact (EI) ion source[21] shows that the most stable isomer in the D0 state has a H-bound geometry, in line with *ab initio* calculations.[14,22,23] This has been interpreted by the fact that resonant photoionization of the π-bonded neutral phenol–Ar precursor complex can generate only the π-bonded structure in the cation due to the Franck–Condon principle. Electron impact ionization does not have such a restriction and can produce the most stable H-bound structure in the cation. The fact that in the cation state the H-bound structure is more stable than the π-bonded isomer implies a π → H switch in the preferred binding motif induced by ionization.[1] This ionization-induced π → H switching reaction has recently been monitored in real time for phenol$^+$···Ar2 by picosecond pump–probe IR spectroscopy.[20,24] Ionization of phenol–Ar2(2π) with two π-bonded Ar ligands triggers a dynamical process, in which one Ar atom

[a] *The Photon Science Institute, The University of Manchester, Alan Turing Building, Oxford Road, Manchester, M13 9PL, UK. E-mail: K.Muller-Dethlefs@manchester.ac.uk*

[b] *Dalton Nuclear Institute, The University of Manchester, Alan Turing Building, Oxford Road, Manchester, M13 9PL, UK*

[c] *School of Chemistry, The University of Manchester, Alan Turing Building, Oxford Road, Manchester, M13 9PL, UK*

[d] *Chemical Resources Laboratory, Tokyo Institute of Technology, 4259 Nagatsuta, Yokohama, 226-8503, Japan. E-mail: mfujii@res.titech.ac.jp*

[e] *Institut für Optik und Atomare Physik, Technische Universität Berlin, Hardenbergstrasse 36, 10623 Berlin, Germany. E-mail: dopfer@physik.tu-berlin.de*

This journal is © the Owner Societies 2011

Phys. Chem. Chem. Phys., 2011, **13**, 6071–6076 | 6071

isomerizes from the π-bound site toward the H-bound site on a time scale of a few picoseconds, with a barrier of less than 100 cm^{-1}. In this paper, we report MATI spectra of phenol$\cdots$Ar$_2(2\pi)$ recorded *via* different intermediate S$_1$ levels involving various degrees of intermolecular vibrational excitation. We also discuss the intermolecular vibrational assignment in the cation ground state, which provides information about geometrical change upon ionization.

2. Experimental details

The experimental setup is essentially the same as that described previously.[25] Briefly, phenol$\cdots$Ar$_2$ clusters were produced in a skimmed supersonic jet expansion of phenol seeded in argon gas at a backing pressure of 2 bar. The heated sample holder (320–340 K) is attached directly to the valve, which operated at a repetition rate of 10 Hz. The resonant excitation and ionization steps of phenol$\cdots$Ar$_2$ clusters were performed by photons from two dye lasers (Radiant Narrowscan) pumped synchronously by a Nd:YAG laser. Coumarin 153 was used as a dye for the first laser (excitation) and a mixture of sulforhodamine B and DCM for the second laser (ionization). The laser frequencies were calibrated accurate to ±0.02 cm^{-1} against the simultaneously recorded iodine absorption spectrum. The counter-propagating laser beams intersected perpendicularly with the molecular beam. A two-photon, two-color (1 + 1′) REMPI spectrum was recorded, employing a fixed frequency of 32 210 cm^{-1} for the ionizing laser in order to ensure soft ionization and reduce fragmentation from higher clusters. The MATI spectra were obtained by fixing the frequency of the excitation laser resonant with a suitable intermediate S$_1$ vibronic state, while the second laser was scanned through successive ionization thresholds to populate long-lived high-n Rydberg states.[17] The prompt photoions produced directly by the laser pulses were separated from the Rydberg states by a 0.5 μs delayed offset field of 1–3 V cm^{-1}. After a further delay of 10–20 μs, a high-voltage pulse of $\sim$300 V cm^{-1} is applied to field-ionize the long-lived Rydberg states and to extract both the spontaneous and MATI ions into the reflectron mass spectrometer.

3. Results

REMPI spectrum

The (1 + 1′) REMPI spectrum of phenol$\cdots$Ar$_2$ shown in Fig. 1 is in good agreement with previous studies[15,18] but displays a significant improvement in the signal-to-noise ratio. The most intense feature in the spectrum at 36282.2 $\pm$ 0.5 cm^{-1} is assigned to the S$_1$ origin (0^0). The additional bands are attributed to vdW vibrational levels. A summary of their frequencies and assignments is reported in Table 1. Fig. 2 visualizes the six possible intermolecular modes of phenol$\cdots$Ar$_2(2\pi)$, which are symmetric and anti-symmetric linear combinations of the intermolecular stretch (σ_s, σ_a), and bend modes along both the x and y directions (β_x, λ_x, β_y, λ_y).
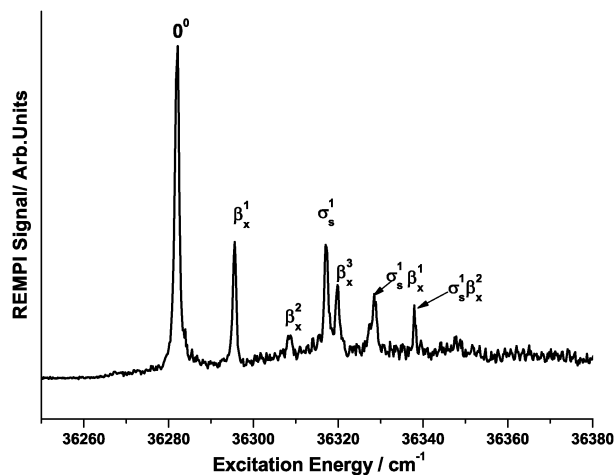

Fig. 1 (1 + 1′) REMPI spectrum of phenol$\cdots$Ar$_2(2\pi)$ of the first electronically excited S$_1$ state. The assignment of the van der Waals modes is included (Table 1).

Table 1 Frequencies and assignment of the intermolecular vibrational bands observed in the REMPI spectrum of the S$_1$ state of phenol$\cdots$Ar$_2(2\pi)$ in Fig. 1

Frequency/cm^{-1}	Assignment
14	β_x^1
27	β_x^2
36	σ_s^1
39	β_x^3
47	$\sigma_s^1\beta_x^1$
57	$\sigma_s^1\beta_x^2$

MATI spectra

Fig. 3 shows the MATI spectrum of phenol$^+\cdots$Ar$_2(2\pi)$, which was obtained *via* the S$_1 0^0$ intermediate state. The weak feature at a total photon energy of 68 288 $\pm$ 5 cm^{-1} is assigned to the field-free adiabatic ionization energy (IE) of phenol$\cdots$Ar$_2(2\pi)$ and is taken as zero internal energy of this structure in the D$_0$ state. In addition, an almost harmonic progression with nearly equal spacing of 10 cm^{-1} is observed (Table 2). The IE value is confirmed by the MATI spectrum recorded *via* the S$_1\beta_x^1$ vibrational state also shown in Fig. 3. In this spectrum the origin of the D$_0$ state (IE) appears with much higher intensity than in the spectrum recorded *via* the S$_1 0^0$ state. This spectrum also displays a progression with spacing of 10 cm^{-1} but with different Franck–Condon intensities. This progression can be divided into two parts with rising and falling intensity of the observed modes. In the first part at low energy the peaks are clearly separated, while they are partially overlapped in the second part, probably due to enhanced spectral congestion. As will be explained below, these peaks are also attributed to the β_x^n van der Waals progression. The progression can be observed up to $n = 8$ (Table 2). In addition, there could be another vibrational progression so far only identifiable as several shoulders in Fig. 3. However, it is presently not possible to commit to an assignment of this progression.

The assignment of the β_x^n van der Waals progression in the MATI spectra *via* the S$_1 0^0$ and S$_1\beta_x^1$ states are confirmed by fitting the experimental intensities to those obtained using
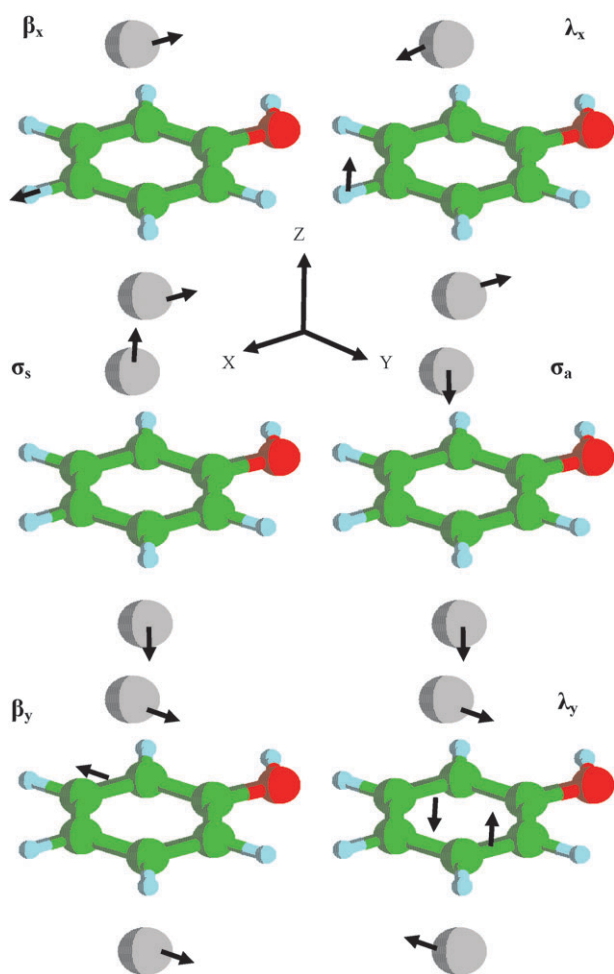
6072 | *Phys. Chem. Chem. Phys.*, 2011, **13**, 6071–6076

This journal is © the Owner Societies 2011

Fig. 2 Intermolecular normal modes of phenol$^{(+)}\cdots Ar_2(2\pi)$.
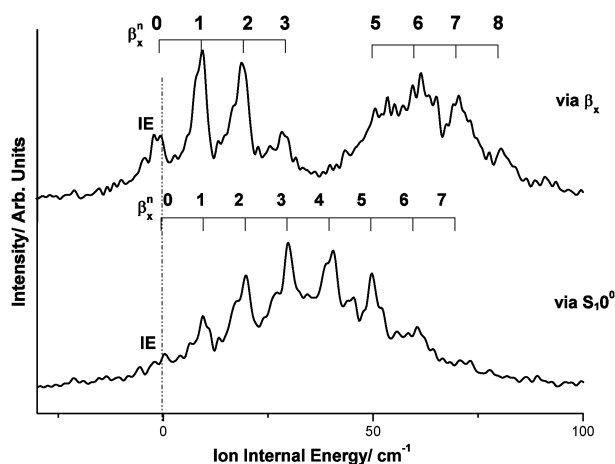
Fig. 3 MATI spectra of phenol$^+\cdots Ar_2(2\pi)$ *via* the $S_1 0^0$ (bottom) and the $S_1\beta_x^1$ (top) intermediate states.

Table 2 Intermolecular vibrational frequencies observed in the MATI spectra of phenol$^+\cdots Ar_2(2\pi)$ *via* the $S_1 0^0$ and $S_1\beta_x^1$ states (Fig. 3)

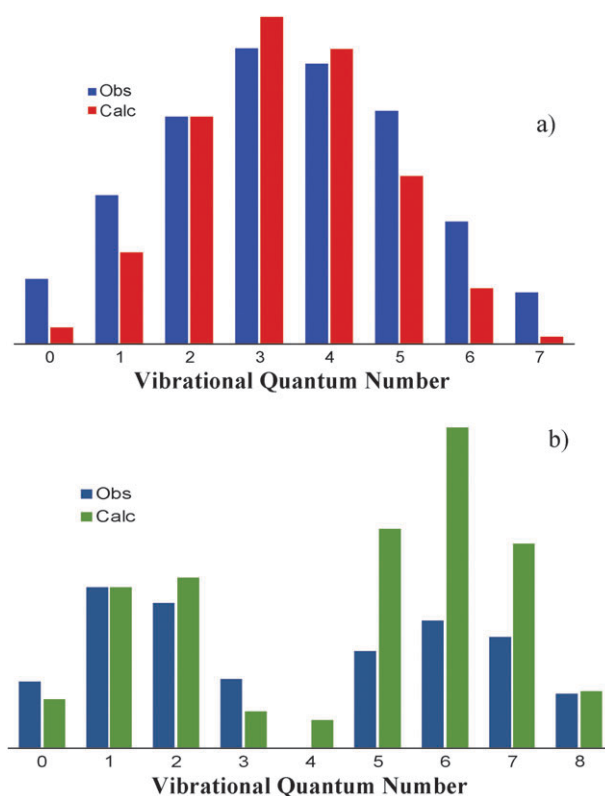| Assignment	Frequency/cm^{-1}	
	via $S_1 0^0$	*via* $S_1\beta_x^1$
β_x^1		
β_x^2	9	9
β_x^3	20	19
β_x^4	30	29
β_x^5	40	50
β_x^6	50	61
β_x^7	61	71
β_x^8	71	81

Fig. 4 Observed and calculated transition intensities of the β_x^n progression in the MATI spectra *via* the $S_1 0^0$ origin (a) and the $S_1\beta_x^1$ state (b).

one-dimensional harmonic Franck–Condon simulations. Fig. 4 compares the observed and calculated transition intensities in the MATI spectrum *via* the $S_1 0^0$ (a) and $S_1\beta_x^1$ (b) states. The transition intensities were obtained by Franck–Condon factors based on harmonic vibrational wavefunctions. The calculated intensities were fit to the observed intensities in the MATI spectrum *via* the $S_1 0^0$ by adjusting a displacement parameter to DL = 0.84, which represents the shift of the potential minima in going from S_1 to the D_0 state in the ion.[26] With the same value of DL = 0.84, the intensity distribution *via* $S_1\beta_x^1$ is well reproduced by the calculated Franck–Condon factors. In particular, the intensity maxima for $n = 2$ and 6 and the minimum at $n = 4$ are nicely recovered by the simulations. The consistent reproduction of the intensity distribution in the β_x^n progression confirms the vibrational assignments. The calculated intensities are slightly stronger for higher vibrational levels, such as $n = 5$–7. This observation may arise from a nonradiative channel, such as dissociation, which opens for the higher vibrational levels, or from limitations to the one-dimensional harmonic Franck–Condon approximation.
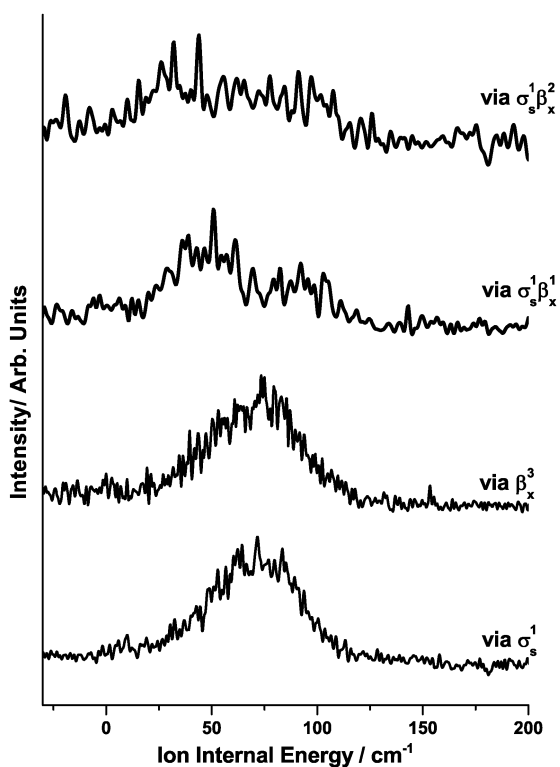
This journal is © the Owner Societies 2011

Phys. Chem. Chem. Phys., 2011, **13**, 6071–6076 | 6073

Fig. 5 MATI spectra of phenol$^+\cdots$Ar$_2(2\pi)$ *via* the S$_1\sigma_s^1$, S$_1\beta_x^3$, S$_1\sigma_s^1\beta_x^1$, and S$_1\sigma_s^1\beta_x^2$ intermediate states.

Fig. 5 shows the MATI spectra recorded *via* the S$_1\sigma_s^1$ and S$_1\beta_x^3$ intermediate states. The IE origin is not observed, and both spectra are characterized by a broad unresolved structure with a maximum at around 75 cm^{-1} internal energy. Even broader structures are observed in the MATI spectra recorded *via* the S$_1\sigma_s^1\beta_x^1$ and S$_1\sigma_s^1\beta_x^2$ intermediate states, as also shown in Fig. 5.

4. Discussion

Vibrational mode assignment in the S$_1$ state

The assignment of S$_1$ intermolecular vibrational structures in Fig. 1 (Table 1) is consistent with the previous assignments.[15,18] To further support this assignment, calculations were performed for the S$_0$ state using the TURBOMOLE package version 5.10.[27] The geometry optimization was performed at the resolution-of-identity second-order Møller–Plesset perturbation theory (RI-MP2) using the aug-cc-pVTZ (Ar) and cc-pVTZ (C, O, H) basis sets and numerical gradients. The calculated frequencies listed in Table 3 confirm the assignment for β_x and σ_s, with experimental/theoretical values of 14/12 and 36/30 cm^{-1}, respectively.

Ionization energy

The IE value can conclusively be assigned as 68 288 ± 5 cm^{-1} by taking the first band in the MATI spectra obtained *via* S$_1$0^0 and S$_1\beta_x^1$. Although the intensity of the IE band as the first member of the β_x^n progression is weak, comparison with the very similar ZEKE spectra of fluorobenzene$^+\cdots$Ar$_2(2\pi)$[4] supports this assignment. In the case of fluorobenzene$^+\cdots$Ar$_2(2\pi)$, a

Table 3 Intermolecular vibrational modes and frequencies in the S$_0$ state of phenol$\cdots$Ar$_2(2\pi)$ calculated at the RI-MP2 level

Mode	Frequency/cm^{-1}
β_x	12
β_y	14
λ_x	25
σ_s	30
λ_x	44
σ_a	45

one-dimensional Franck–Condon simulation confirmed the intensity distribution of the β_x^n progression and the assignment of the n quantum number to the individual vibrational transitions, including $n = 0$ for the IE band.

The IE of phenol$^+\cdots$Ar$_2(2\pi)$ is redshifted by ΔIE = -340 cm^{-1} from the IE of phenol$^+$.[28] This shift is almost twice the red-shift for the phenol$^+\cdots$Ar(π) dimer (ΔIE = -176 cm^{-1}).[17] This observation indicates the similarity of the intermolecular bonding type in phenol$^{(+)}\cdots$Ar(π) and phenol$^{(+)}\cdots$Ar$_2(2\pi)$. This relationship reflects the same trend as already observed in the case of aniline$^{(+)}\cdots$Ar$_n(n\pi)$[7] and fluorobenzene$^{(+)}\cdots$Ar$_n(n\pi)$[5] with $n \leq 2$, where the additivity rule also holds almost strictly, ΔIE = -111 ($n = 1$) and -219 ($n = 2$) cm^{-1} for aniline, and ΔIE = -223 ($n = 1$) and -422 ($n = 2$) cm^{-1} for fluorobenzene.

Vibrational mode assignment in the D$_0$ state

The structure of the progression with a spacing of 10 cm^{-1} observed in the MATI spectrum *via* the S$_1$0^0 state of phenol$\cdots$Ar$_2(2\pi)$ is similar to those seen in aniline$^+\cdots$Ar$_2(2\pi)$,[7] benzonitrile$^+\cdots$Ar$_2(2\pi)$,[3] and fluorobenzene$^+\cdots$Ar$_2(2\pi)$.[4] The vibrational spacing was found to be 9 cm^{-1} for the case of benzonitrile and fluorobenzene, and 11 cm^{-1} for aniline. In all these A$^+\cdots$Ar$_2(2\pi)$ clusters the fundamental mode of these progressions was assigned to the symmetric bending mode, β_x. In analogy, the vibrational progressions in the MATI spectra of phenol$^+\cdots$Ar$_2(2\pi)$ *via* S$_1$0^0 and S$_1\beta_x^1$ are also assigned to β_x^n. This interpretation supports the β_x assignment in the S$_1$ state, because the MATI spectrum *via* S$_1\beta_x^1$ displays also the progression of the β_x^n mode but with different Franck–Condon intensities.

The MATI spectrum of phenol$^+\cdots$Ar(π) *via* the S$_1$0^0 state shows a harmonic progression in b_x^n (15, 31, 46 cm^{-1} for $n = 1$–3).[18] The ratio of b_x/β_x observed in phenol$^+\cdots$Ar$_n(n\pi)$ for $(n = 1)/(n = 2)$ of 15/10 is similar to the case of isoelectronic aniline (16/11).[7] These ratios are slightly larger than those observed for fluorobenzene and benzonitrile (12/9).[3,4] The b_x and β_x assignments for phenol$^+\cdots$Ar$_n(n\pi)$ with $n = 1$ and 2 can be further confirmed by considering the following simple model.[6] The reduced masses μ_{b_x} and μ_{β_x} for the vibrational modes b_x and β_x are given by eqn (1) and (2),

$$\mu_{b_x} = (1/mR_0^2 + 1/MR_0^2 + 1/I_{yy})^{-1} \qquad (1)$$

$$\mu_{\beta_x} = (1/mR_0^2 + 2/MR_0^2)^{-1} \qquad (2)$$

where M and m are the masses of phenol and Ar, respectively, I_{yy} is the moment of inertia of phenol with respect to the y axis, and R_0 is the equilibrium center-of-mass distance between

6074 | *Phys. Chem. Chem. Phys.*, 2011, **13**, 6071–6076

This journal is © the Owner Societies 2011

Table 4 Structural parameters for phenol$^{+}\cdots$Ar(π) and phenol$^{+}\cdots$Ar$_2$(2π)

M/u	94
M/u	40
R_0/Å[22]	3.3
I_{yy}[29]	193
MR_0^2/uÅ^2	1024
mR_0^2/uÅ^2	436
μ_{b_x}/u	125
μ_{β_x}/u	250
ν_{b_x}/cm^{-1}	15
ν_{β_x}/cm^{-1}	10

phenol and Ar. The frequencies ν_{b_x} and ν_{β_x} of the b_x and β_x modes are then given by eqn (3) and (4),

$$\nu_{b_x} = (1/2\pi)(k_{\phi\phi}^{b_x}/\mu_{b_x})^{1/2} \qquad (3)$$

$$\nu_{\beta_x} = (1/2\pi)(k_{\phi\phi}^{\beta_x}/\mu_{\beta_x})^{1/2} \qquad (4)$$

where $k_{\phi\phi}^{b_x}$ and $k_{\phi\phi}^{\beta_x}$ are the force constants for the b_x and β_x modes, respectively. The angle ϕ represents the angle between the y axis and the vector connecting Ar and the center-of-mass of phenol. Under the reasonable assumption that the two force constants are equal, the ratio of the two bending frequencies is given by the equation:

$$\nu_{\beta_x}/\nu_{b_x} = (\mu_{b_x}/\mu_{\beta_x})^{1/2} \qquad (5)$$

For phenol$^{+}\cdots$Ar(π) and phenol$^{+}\cdots$Ar$_2$(2π) eqn (5) holds very well when using the values as listed in Table 4. For both sides of eqn (5) we obtain 0.7, which means that the force constants $k_{\phi\phi}^{\beta_x}$ and $k_{\phi\phi}^{b_x}$ are essentially identical, supporting again the vibrational mode assignments. The broad structures observed in the MATI spectra recorded via $S_1\sigma_s^1$, $S_1\beta_x^3$, $S_1\sigma_s^1\beta_x^1$, and $S_1\sigma_s^1\beta_x^2$ (Fig. 5) do not give any further information on the vibrational modes in the D_0 state of phenol$^{+}\cdots$Ar$_2$(2π).

The simple one-dimensional harmonic Franck–Condon simulation yields a displacement value of $D = 3.45$ for the shift of the potential minima of phenol$^{(+)}\cdots$Ar$_2$(2π) along the β_x coordinate upon ionization ($D_0 \leftarrow S_1$). Despite this rather simple model, the relative intensities of the β_x^n progressions in the MATI spectra in Fig. 3 can be reproduced surprisingly well. Similarly to previous studies on related systems,[3,4,7] this displacement value can directly be converted,[7] for phenol$^{(+)}\cdots$Ar$_2$(2π), into a change in the equilibrium bond angle along the β_x normal coordinate, yielding a value of $\Delta\phi_{\beta_x} = 9.1°$. Interestingly, this value is slightly larger than the corresponding values obtained for isoelectronic aniline$^{(+)}\cdots$Ar$_2$ ($8.8°$)[7], fluorobenzene$^{(+)}\cdots$Ar$_2$ ($6°$)[4], and benzonitrile$^{(+)}\cdots$Ar$_2$ ($6°$).[3] At this stage, it is, however, rather difficult to extract more quantitative information about the actual changes in the potential energy surface in phenol$^{(+)}\cdots$Ar$_2$(2π) upon ionization due to the severe limitations of the employed harmonic one-dimensional model, which for example neglects the effects of anharmonicity and inter-molecular mode mixing arising from Duschinsky rotation. Moreover, as the reaction coordinate for the $\pi \rightarrow$ H switching reaction is not completely established,[14,23] the current result provides only approximate information about the energetics of this isomerization process (e.g., the barrier height).

5. Concluding remarks

The MATI spectra of phenol$^{+}\cdots$Ar$_2$(2π) recorded via the different S_1 intermediate states were analyzed and the ionization energy could be determined to be $68\,288 \pm 5$ cm^{-1}. The observed progression in the MATI spectrum via the S_10^0 intermediate state shows a strong similarity with those of other monosubstituted benzene clusters with Ar (e.g., fluorobenzene, benzonitrile, aniline). The fundamental mode was assigned to the symmetric bending vibrational mode β_x with a frequency of 10 cm^{-1}. The long progression in the β_x mode indicates a strong change of the geometry upon ionization along this coordinate, which is confirmed by one-dimensional harmonic simulations of the Franck–Condon intensities. Upon ionization, the Ar atoms are more attracted toward the OH group of phenol.

Acknowledgements

References

1 O. Dopfer, Z. Phys. Chem. (Muenchen, Ger.), 2005, **219**, 125.
2 T. Kobayashi, K. Honma, O. Kajimoto and S. Tsuchiya, J. Chem. Phys., 1987, **86**, 1111.
3 M. Araki, S. Sato and K. Kimura, J. Phys. Chem. A, 1996, **100**, 10542.
4 H. Shinohara, S. Sato and K. Kimura, J. Phys. Chem. A, 1997, **101**, 6736.
5 G. Lembach and B. Brutschy, J. Chem. Phys., 1997, **107**, 6156.
6 E. J. Bieske, M. W. Rainbird, I. M. Atkinson and A. E. Knight, J. Chem. Phys., 1989, **91**, 752.
7 M. Takahashi, H. Ozeki and K. Kimura, J. Chem. Phys., 1992, **96**, 6399.
8 E. J Bieske, M. W. Rainbird and A. E. Knight, J. Chem. Phys., 1991, **94**, 7019.
9 Q. Gu and J. L. Knee, J. Chem. Phys., 2008, **128**, 064311.
10 M. Becucci, G. Pietraperzia, N. M. Lakin, E. Castellucci and Ph. Bréchignac, Chem. Phys. Lett., 1996, **260**, 87.
11 M. S. Ford, S. R. Haines, I. Pugliesi, C. E. H. Dessent and K. Müller-Dethlefs, J. Electron Spectrosc. Relat. Phenom., 2000, **112**, 231.
12 T. Ebata, A. Iwasaki and N. Mikami, J. Phys. Chem. A, 2000, **104**, 7974.
13 G. V. Hartland, B. F. Henson, V. A. Venturo and P. M. Felker, J. Phys. Chem., 1992, **96**, 1164.
14 J. Černy, X. Tong, P. Hobza and K. Müller-Dethlefs, J. Chem. Phys., 2008, **128**, 114319.
15 S. Ishiuchi, Y. Tsuchida, O. Dopfer, K. Müller-Dethlefs and M. Fujii, J. Phys. Chem. A, 2007, **111**, 7569.
16 I. Kalkman, C. Brand, T. B. C. Vu, W. L. Meerts, Y. N. Svartsov, O. Dopfer, X. Tong, K. Müller-Dethlefs, S. Grimme and M. Schmitt, J. Chem. Phys., 2009, **130**, 224303.

17 C. E. H. Dessent, S. R. Haines and K. Müller-Dethlefs, *Chem. Phys. Lett.*, 1999, **315**, 103.
18 S. R. Haines, C. E. H. Dessent and K. Müller-Dethlefs, *J. Electron Spectrosc. Relat. Phenom.*, 2000, **108**, 1.
19 N. Gonohe, H. .Abe, N. Mikami and M. Ito, *J. Phys. Chem.*, 1985, **89**, 3642.
20 S. Ishiuchi, M. Sakai, Y. Tsuchida, A. Takeda, O. Dopfer, K. Müller-Dethlefs and M. Fujii, *J. Chem. Phys.*, 2007, **127**, 114307.
21 N. Solcà and O. Dopfer, *J. Phys. Chem. A*, 2001, **105**, 5637; N. Solcà and O. Dopfer, *Chem. Phys. Lett.*, 2003, **369**, 68.
22 J. Çerny, X. Tong, P. Hobza and K. Müller-Dethlefs, *Phys. Chem. Chem. Phys.*, 2008, **10**, 2780.
23 N. Solcà and O. Dopfer, *J. Mol. Struct.*, 2001, **563/564**, 241.
24 S. Ishiuchi, M. Sakai, Y. Tsuchida, A. Takeda, Y. Kawashima, M. Fujii, O. Dopfer and K. Müller-Dethlefs, *Angew. Chem., Int. Ed.*, 2005, **44**, 6149.
25 S. R. Haines, W. D. Geppert, D. M. Chapman, M. J. Watkins, C. E. H. Dessent, M. C. R. Cockett and K. Müller-Dethlefs, *J. Chem. Phys.*, 1998, **109**, 9244.
26 E. Hutchisson, *Phys. Rev.*, 1930, **36**, 410.
27 R. Ahlrichs, M. Bär, M. Häser, H. Horn and C. Kölmel, *Chem. Phys. Lett.*, 1989, **162**, 165.
28 O. Dopfer, PhD thesis, Technische Universität München, 1994.
29 E. Mathier, D. Welti, A. Bauder and Hs. H. Günthard, *J. Mol. Spectrosc.*, 1971, **37**, 63.